Astron. Astrophys. 317, L31–L34 (1997)

ASTRONOMY AND ASTROPHYSICS

LETTER

Thermal birth below the sonic point of turbulent streams in the solar wind

R. Grappin J. Léorat E. Cavillier G. Prigent

DAEC, Observatoire de Paris, Université Paris VII, CNRS (UA 173), F-92195 Meudon Cedex and ASCI, F-91400 Orsay, France

Received 19 September 1996 / Accepted 8 October 1996

Abstract. We study the loss of stability of streams in the region of acceleration of the solar wind. We solve the Euler equations in spherical coordinates with open boundaries. We assume here axisymmetry, temperature conservation during advection, and neglect the magnetic field. We show that any initial velocity modulation vanishes with distance when the inner boundary temperature is uniform, while a persistent stream structure obtains in presence of a temperature modulation at the inner boundary. The stream structure is shown to be unstable in the region where the expansion rate is significantly smaller than the nonlinear time, i.e., below the sonic point. Two observational features are recovered: the correlation between temperature and radial velocity fluctuations (which persits in spite of the turbulence at stream interface), and a trend towards pressure equilibrium (Marsch and Tu, 1993).

Key words: Sun: solar wind – Hydrodynamics – turbulence – Methods: numerical

1. Introduction

The origin and evolution of the turbulent spectrum in the solar wind observed in situ has been the object of much attention (Tu and Marsch, 1995); the classical scenario is an MHD version of the Richardson-Kolmogorov cascade: velocity gradients provided by the largest scales (here the stream structure) generate temporal fluctuations, which in turn generate smaller scales velocity gradients etc... (Coleman, 1968). The expansion of the solar wind plasma, due to the main radial flow, is not taken into account in this description. However, it has been shown recently that the expansion strongly limits nonlinear interactions and may prevent the spectral formation (Grappin and Velli, 1996). As a consequence, the spectrum should form close to the sun, in a region where the expansion rate is smaller. In order to cope with this problem, one must take gravity into account, curvature, and consider open boundaries, in contrast with the periodic conditions used currently in turbulence simulations.

Close to the sun, the temperature and the magnetic field should play an important role, contrary for instance to the ecliptic, far-sun situation where the stream shear provides the largest energy reservoir. We consider in this preliminary work the role of temperature fluctuations, postponing for future work the study of the role of the magnetic field and three-dimensionality. We integrate for this purpose the Navier-Stokes equations with central gravity, including the sonic radius (or region) within the domain. We consider the axisymmetric case, with a polytropic index $\gamma = 1$, inspired by the high thermal conductivity along the radial magnetic field lines.

Why temperature fluctuations? As shown by Parker (1958) in the isotropic (spherically symmetric) situation, the temperature of the plasma determines the position of the sonic radius. We show below that this isotropic solution is extremely stable, that is, any initial velocity shear (i.e., seed of radial streams) imposed close to the sun vanishes rapidly with distance in the isothermal case; on the contrary, temperature fluctuations imposed at the coronal level lead to persistent streams with shear increasing with distance, which are eventually unstable. We investigate the evolution of such a collection of streams close to the sun, and examine whether this simple model may help to shed some light on the mechanism of formation of turbulence in the accelerating solar wind.

2. Method

The axisymmetric equations for density r, velocity u and temperature T read in spherical coordinates r, θ, ϕ:

$$\frac{\partial u_r}{\partial t} + u_r\frac{\partial u_r}{\partial r} + \frac{u_\theta}{r}\frac{\partial u_r}{\partial \theta} - \frac{u_\theta^2}{r} = -\frac{1}{\rho}\frac{\partial P}{\partial r} - \frac{GM}{r^2} \quad (1)$$

$$\frac{\partial u_\theta}{\partial t} + u_r\frac{\partial u_\theta}{\partial r} + \frac{u_\theta}{r}\frac{\partial u_r}{\partial \theta} - \frac{u_\theta u_r}{r} = -\frac{1}{r\rho}\frac{\partial P}{\partial \theta} \quad (2)$$

$$\frac{\partial \rho}{\partial t} + \frac{\partial(\rho u_r)}{\partial r} + \frac{\partial(\rho u_\theta)}{r\partial\theta} + \frac{\rho u_\theta cot\theta}{r} + 2\frac{\rho u_r}{r} = 0 \quad (3)$$

$$\frac{\partial T}{\partial t} + u_r\frac{\partial T}{\partial r} + \frac{u_\theta}{r}\frac{\partial T}{\partial \theta} = 0 \quad (4)$$

Send offprint requests to: R. Grappin; Observatoire de Paris, F-92195 Meudon Cedex, France

where $P = \rho T$ is the pressure. The velocity unit is the sound velocity $c_0 = \sqrt{T_0}$ associated with a standard temperature; unit distance is twice the sonic radius $r^\star = GM/(2c_0^2)$. The numerical domain is a spherical sector around the equator, $[r_0, r_1] \star [\pi/2 - \Delta\theta/2, \pi/2 + \Delta\theta/2]$. In the following runs, the angular width $\Delta\theta$ is $\pi/4$, the inner and outer shells radii are $r_0 = 0.25$ and $r_1 = 1.21$. When T = 1 everywhere, the flow is thus subsonic for $0.25 \leq r \leq 0.5$ and supersonic for $0.5 \leq r \leq 1.21$. The resolution is 540 (radial direction) by 180 (latitude).

Gradients are computed via compact finite differences of order 6 within the domain and of order 4 at the boundaries, and dissipation at the grid-scale is obtained via a filter every five time-steps (Lele, 1992). The temporal scheme is Runge-Kutta of order 3. At the latitude boundaries we assume even density, radial velocity and temperature, and an odd poloidal velocity component. This results from axisymmetry when $\Delta\theta = \pi$; when $\Delta\theta < \pi$, it amounts to assuming free-slip conditions at the latitudinal boundaries. The radial boundary conditions are imposed via characteristics (Thompson, 1987, Poinsot and Lele, 1993): no conditions are imposed at the outer boundary where the flow is supersonic; the temperature profile and a zero incoming flux of acoustic waves are imposed at the inner boundary. A last condition is needed; except for the first two experiments for which $u_\theta(r_0, \theta) = 0$ (runs Z1 and Z2 below), we will use $\frac{\partial T}{\partial r} + c\frac{\partial u_\theta}{\partial r} = 0$ at the inner boundary. All runs start from a stationary, spherically symmetric transonic wind prepared with temperature $T = 1$ (see Grappin Cavillier and Velli, 1996), but to which (with one exception described immediately below) we apply a nonuniform temperature profile, which is maintained at the inner shell. The temperature changes lead to acceleration or deceleration, depending on the local sign of the variation. Transient perturbations are first swept out of the domain and a new flow regime sets in.

3. Results

The first two experiments (figure 1) demonstrate the impossibility to obtain persistent shear flows by directly imposing the velocity shear itself at the inlet, in contrast to standard (i.e., homogeneous and gravitationless) numerical experiments of shear flows. In run Z1, we impose at the inner boundary a cold latitudinal band imbedded within two warm regions, which leads after some time to a stationary slow and cold stream, in between two warm, fast flows. As shown by figure 1a, the velocity contrast between streams increases clearly with distance. In run Z2, we restart the computation from the latter flow regime, but changing two features: we replace the inhomogeneous temperature field by a uniform one, while fixing the velocity shear at the inner boundary to be the preceding stationary profile. As figure 1b shows, after some crossing times, another stationary regime obtains, in which now the velocity contrast decreases with distance and isotropy is almost recovered at the outlet. Note that, in order to allow for easier comparison between the two runs, we have imposed a zero transverse velocity u_θ at the inner boundary. This condition is relaxed, as mentioned above, in the rest of the paper.

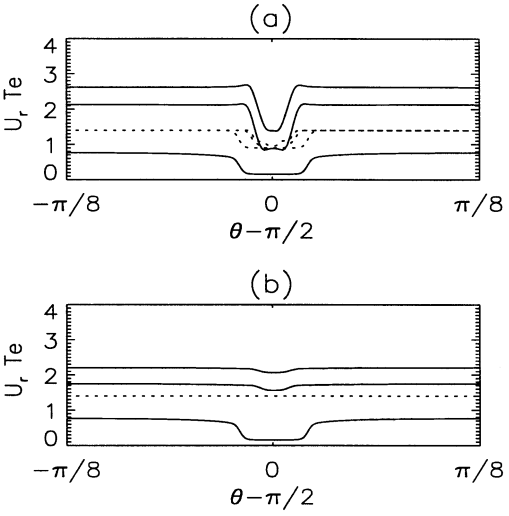

Fig. 1. Shear flows resulting from fixing either the velocity or the temperature at the inner boundary. Transverse profiles of radial velocity (continuous), temperature (dotted), at three distances: inner shell, middle of the domain, and outer shell. (a) run Z1: Fixed temperature profile at the inner shell (b) run Z2: Fixed velocity profile, but uniform temperature field.

In the following two experiments, the northern latitudes ($\theta < \pi/2$) are colder ($T = T_{min}$) than the southern ($\theta > \pi/2, T = T_{max}$). The flow for $T_{min} = 1$ and $T_{max} = 1.5$ is shown in figure 2 (run A); it is stationary. Note that, since $\gamma = 1$, lines of constant temperature trace fluid particles; in particular, the stream boundary is shown by plotting isothermals with intermediate values (fig.2b). Several features are remarkable and will be found again in the subsequent experiments: a) the velocity and temperature profiles are well correlated b) the density and temperature profiles are anticorrelated c) the stream boundary is not radial, as the cold stream is "pushed" aside by the warm stream.

In order to demonstrate how stability is lost when the expansion rate of the wind is decreased, we consider a lower temperature profile (run B: $T_{min} = 0.8$ and $T_{max} = 1.3$). This decreases the mean flow without decreasing the shear. Figure 3 shows that after several advection times the interface now shows a series of quasi-periodic vortices. Another factor which may destabilize the flow is the "pressure" the warm streams exert on the cold streams. If a cold stream lies in between two warm streams, the latter should pinch the cold stream and bring the two interfaces with opposite vorticity in closer contact, hence increasing nonlinear interactions. In Figure 4 (run C: $T_{min} = 1$, $T_{max} = 1.5$), eddies indeed appear where the two interfaces become close together; they later detach from the interface, similarly to a von Karman street in a wake. The contact must form not too far (this depends on the angular size of the cold stream), otherwise expansion prevents the von Karman street from appearing. Notice that in this run the radial velocity profile shows at the inner boundary a dissymetry between the two interfaces which pro-

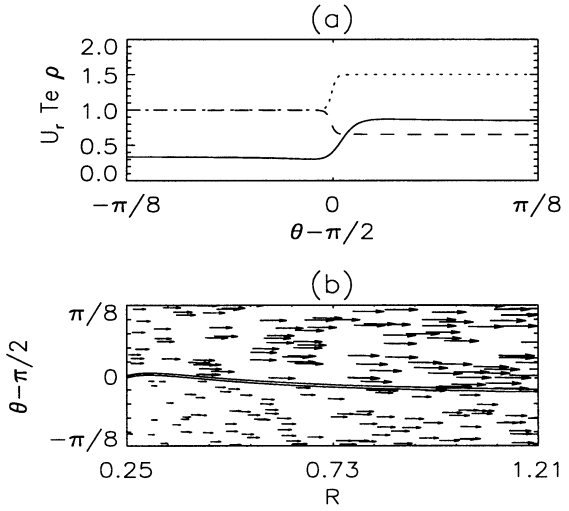

Fig. 2. Shear flow layer induced by a temperature step imposed at the inner boundary (run A, time t = 1.5). (a) transverse profiles at the inner shell of radial velocity (continuous), temperature (dotted) and density (dashed). (b) Flow in the (r, θ) domain: velocity field and (1.1, 1.4) isothermals.

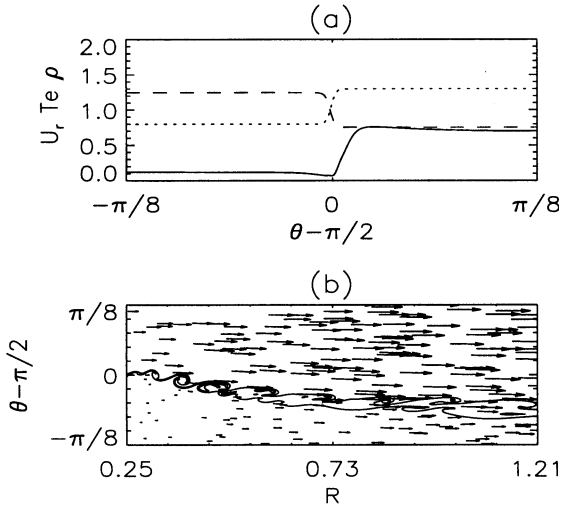

Fig. 3. Shear flow layer with lower temperature (run B, t = 1.5). Same legend as figure 2, but for (b): isothermals are (.9, 1.2).

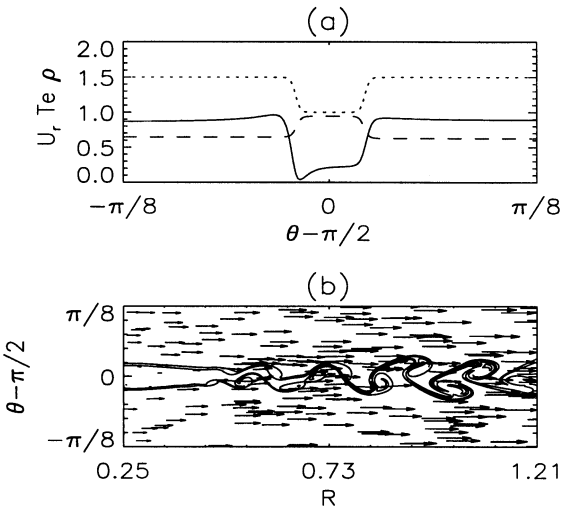

Fig. 4. Von-Karman street resulting from a cold equatorial region imbedded between two warm regions (run C). Same legend as in figure 2.

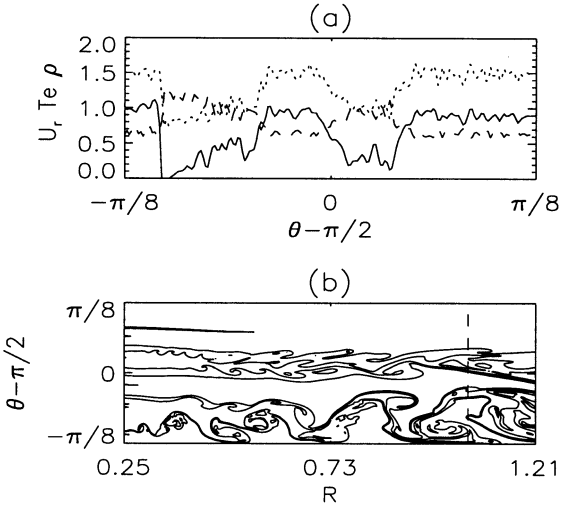

Fig. 5. (run D, t = 2.5) Two cold regions imbedded in three warm regions. Same legend as in figure 2 (without velocity field).

vides a seed for the sinuous instability; on the contrary, the von Karman street does not develop (with the parameters adopted here) when u_θ is set to zero at the inner boundary, which is one of the ways to impose symmetry, as done in runs Z1 and Z2 (see figure 1).

In the real solar wind, a whole spectrum of fluctuations is excited. Can this result from a spectrum of thermal fluctuations in the corona? To gain some insight on this question we build a temperature spectrum by adding a white noise to a set of two cold regions imbedded within three warm regions (run D: figure 5). One sees that this temperature profile generates a similar radial velocity profile (fig.5a), which destabilizes downstream (figure 5b).

4. Discussion

The last experiment shows that, to obtain a spectrum of radial velocities resembling the one observed at several tens of solar radii, it is necessary and sufficient, in the framework of the present simplified hydrodynamic model, to impose below the sonic point a steady temperature spectrum with moderate fluctuation amplitudes (50%) at the coronal level. Each sub-region with a given temperature gives rise to a flux tube with its own sonic distance, i.e., its own sub-stream. There are some interactions between flux tubes during advection, so that, even if the interfaces remain laminar, there are deviations from a simple extrapolation of Parker's phenomenology. But even far from the inner radius, the radial velocity profile still reflects the complex temperature profile at the inner boundary (figure 6a). A second feature is that the density profile is anti-correlated with

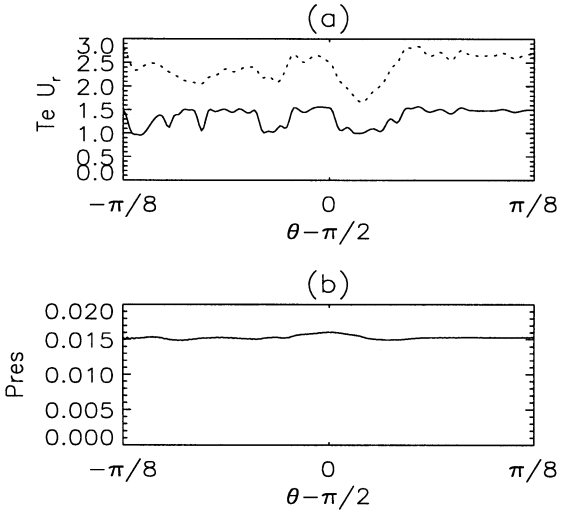

Fig. 6. (run D, t = 2.5). Transverse profiles at r = 1.05 (along the vertical dashed line in figure 5) (a) temperature (continuous) and radial velocity (dashed) (b) pressure.

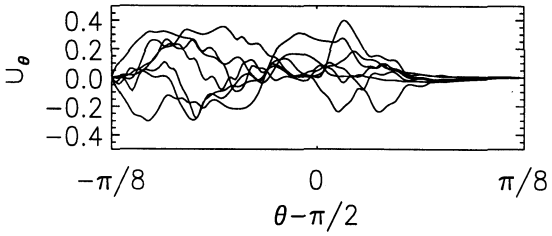

Fig. 7. (run D, t = 1.5, 1.75, ...3). Successive transverse profiles of the transverse velocity at r = 1.05 (see vertical dashed line in figure 5).

the temperature profile, corresponding to an approximate transverse pressure equilibrium, almost devoid of acoustic waves (figure 6b); this is reminiscent of the balance between kinetic and magnetic pressure met in observational data (see Marsch and Tu, 1993). Note that the latter point depends largely on boundary conditions, as acoustic waves are strongly amplified during their propagation through the low-expansion region (see Grappin et al., 1996). If the interfaces are unstable, the (U_r, T) correlation is destroyed, the amount of de-correlation measuring the amount of "interface turbulence" which occured during advection: figure 7 gives an idea of the temporal fluctuations of the transverse velocity at the same radius as figure 6.

Our present model is idealized in three main points: (i) The evolution of the interface might change deeply by considering fully three-dimensional simulations: for example, it is known that in homogeneous shear flows, the transition to the third dimension changes the evolution of eddies which break into pieces instead of merging. (ii) On the other hand, it is probable (Siregar et al., 1994) that the magnetic field will moderate the interface instability exhibited e.g. in figure 5. Note however that the present work (in particular figure 1) shows that the results obtained in homogeneous simulations cannot be easily extrapolated to the accelerating wind. (iii) What would be the result of relaxing the polytropic (γ = 1) assumption? This is clearly a persistent challenge, even in the isotropic case, and a fully consistent solution might be outside the fluid framework. However, we feel that further study of the polytropic model as mentioned in (i) and (ii), now in progress, should help understanding the birth of turbulence in the solar wind.

We thank M. Velli, A. Mangeney and E. Marsch for fruitful discussions and IDRIS for providing the computer facilities.

References

Coleman, P. J., ApJ , 153, 371, 1968.
Grappin, R., and Velli M., J. Geophys. Res., 101, 425, 1996.
Grappin R., Cavillier E. and Velli M., Propagation of acoustic waves in isothermal winds in the vicinity of the sonic point, A&A , to appear, 1996.
Lele, S.K., J. Comput. Phys. 103, 16-42, 1992.
Marsch, E., Tu C.-Y., Ann. Geophys., 11, 659, 1993.
Parker, E.N., ApJ , 128, 664, 1958.
Poinsot T.J. and Lele S.K., J. Comput. Phys., 101, 104, 1993.
Siregar, E., Stribling W.T., and Goldstein M.L., Phys. Plasmas, 1, 2125, 1994.
Thompson, K.W., J. Comput. Phys., 68, 1-15, 1987.
Tu, C.-Y. and Marsch E., Space Sci. Rev., 73, 1, 1995.

This article was processed by the author using Springer-Verlag LaTeX A&A style file *L-AA* version 3.